

# An Engineered Old Yellow Enzyme that Enables Efficient Synthesis of (4*R*,6*R*)-Actinol in a One-Pot Reduction System

Shoichiro Horita,<sup>[a]</sup> Michihiko Kataoka,<sup>[b]</sup> Nahoko Kitamura,<sup>[c]</sup> Takuya Nakagawa,<sup>[c]</sup> Takuya Miyakawa,<sup>[a]</sup> Jun Ohtsuka,<sup>[a]</sup> Koji Nagata,<sup>[a]</sup> Sakayu Shimizu,<sup>[c]</sup> and Masaru Tanokura\*<sup>[a]</sup>

(4*R*,6*R*)-Actinol can be stereo-selectively synthesized from ketoisophorone by a two-step conversion using a mixture of two enzymes: *Candida macedoniensis* old yellow enzyme (CmOYE) and *Corynebacterium aquaticum* (6*R*)-levodione reductase. However, (4*S*)-phorenol, an intermediate, accumulates because of the limited substrate range of CmOYE. To address this issue, we solved crystal structures of CmOYE in the presence and absence of a substrate analogue *p*-HBA, and introduced point mutations into the substrate-recognition loop. The most effec-

tive mutant (P295G) showed two- and 12-fold higher catalytic activities toward ketoisophorone and (4*S*)-phorenol, respectively, than the wild-type, and improved the yield of the two-step conversion from 67.2 to 90.1%. Our results demonstrate that the substrate range of an enzyme can be changed by introducing mutation(s) into a substrate-recognition loop. This method can be applied to the development of other favorable OYEs with different substrate preferences.

## Introduction

Biocatalytic conversion using enzyme(s) is a promising technique for the preparation of optically active compounds because of their high enantioselectivity and substrate specificity. However, the strict specificity sometimes results in a limited substrate range, such that biocatalytic conversion is not always applicable for the synthesis of target molecules. If a strategy to create enzymes with broader substrate range can be established, biocatalytic conversion will become a more useful tool for the synthesis of various optically active compounds. Recently, iterative saturation mutagenesis (ISM) has been reported as a promising strategy to design artificial enzymes for biocatalytic conversion.<sup>[1]</sup> This method is an efficient approach for the directed evolution of functional enzymes by performing iterative cycles of high-throughput saturation mutagenesis at rationally chosen sites.<sup>[1]</sup>

Proteins of the old yellow enzyme (OYE) family are potential targets for protein engineering for useful biocatalysts, as they catalyze the asymmetric reduction of C=C bonds in  $\alpha,\beta$ -unsaturated carbonyl compounds with high enantioselectivity (molecular mechanisms below). Several trials have been performed for changing the enantioselectivity and/or substrate range of OYE proteins with linear or cyclic enone compounds.<sup>[2,3]</sup>

Recently, some OYE proteins were also reported to be of use in multi-step asymmetric reduction in combination with other biocatalysts.<sup>[4]</sup> (4*R*,6*R*)-4-Hydroxy-2,2,6-trimethylcyclohexanone ((4*R*,6*R*)-actinol) is an industrially important doubly chiral building block useful for the synthesis of xanthoxin, zeaxanthin, and related compounds.<sup>[4]</sup> A separate two-step biocatalytic conversion method has been established to synthesize (4*R*,6*R*)-actinol from the commercially available compound 2,6,6-trimethylcyclohex-2-ene-1,4-dione (ketoisophorone).<sup>[4,5]</sup> In this method, ketoisophorone is first reduced to (6*R*)-2,2,6-trimethyl-1,4-cyclohexanedione ((6*R*)-levodione) by *Saccharomyces cerevisiae* OYE (ScOYE2)<sup>[6]</sup> or *Candida macedoniensis* AKU4588 (CmOYE),<sup>[7]</sup> and (6*R*)-levodione is then reduced to (4*R*,6*R*)-actinol by (6*R*)-levodione reductase from *Corynebacterium aquaticum* M-13 (LVR)<sup>[8,9]</sup> (upper pathway in Scheme 1).<sup>[4]</sup>

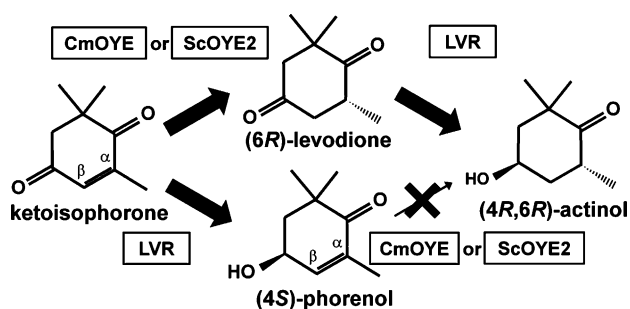
To establish a more cost-effective and environmentally friendly, synthetic method for (4*R*,6*R*)-actinol, we developed a one-pot system for this two-step biocatalytic conversion. However, when the two-step biocatalytic conversion was performed in one pot with a mixture of ScOYE2 and LVR, the yield of (4*R*,6*R*)-actinol was only 16%, with an accumulation of an intermediate, 4-hydroxy-2,6,6-trimethyl-2-cyclohexanone ((4*S*)-phorenol)<sup>[4]</sup> in 48% yield, a result of the inefficient reduction of (4*S*)-phorenol to (4*R*,6*R*)-actinol by ScOYE2. When CmOYE was used instead of ScOYE2, the yield of (4*R*,6*R*)-actinol increased

[a] Dr. S. Horita, Dr. T. Miyakawa, Dr. J. Ohtsuka, Dr. K. Nagata, Prof. Dr. M. Tanokura  
Department of Applied Biological Chemistry  
Graduate School of Agricultural and Life Sciences  
University of Tokyo  
1-1-1 Yayoi, Bunkyo-ku, Tokyo 113-8657 (Japan)  
E-mail: amtanok@mail.ecc.u-tokyo.ac.jp

[b] Prof. Dr. M. Kataoka  
Division of Applied Life Sciences  
Graduate School of Life and Environmental Sciences  
Osaka Prefecture University  
1-1 Gakuencho, Naka-ku, Sakai, Osaka 599-8531 (Japan)

[c] N. Kitamura, T. Nakagawa, Prof. Dr. S. Shimizu  
Division of Applied Life Sciences  
Graduate School of Agriculture, Kyoto University  
Oiwake, Kitashirakawa, Sakyo-ku, Kyoto 606-8502 (Japan)

Supporting information for this article is available on the WWW under <http://dx.doi.org/10.1002/cbic.201402555>.



**Scheme 1.** Two-step biocatalytic conversion of ketoisophorone to (4*R*,6*R*)-actinol. Biocatalytic synthesis of (4*R*,6*R*)-actinol from ketoisophorone is performed by CmOYE (or ScOYE2) and LVR. CmOYE and ScOYE2 show less catalytic activity in the reduction of (4*S*)-phorenol than in the other reactions.

to 67.2%, but 28.1% still remained as (4*S*)-phorenol (this study).

The molecular mechanism of asymmetric reduction by OYEs has been elucidated in detail.<sup>[10–13]</sup> In brief, a strictly conserved histidine/asparagine or histidine/histidine pair<sup>[11]</sup> and a tyrosine residue<sup>[12]</sup> are involved in the asymmetric reduction; a hydride derived from FMNH<sub>2</sub> is stereo-selectively transferred to C<sup>β</sup> of the bound  $\alpha,\beta$ -unsaturated carbonyl compound, and the tyrosine residue donates a proton to C<sup>α</sup> of the  $\alpha,\beta$ -unsaturated carbonyl compound from the opposite side. However, the structural basis of the different substrate preferences was unknown.

To gain insight into the structural basis of the substrate recognition, we solved structures of CmOYE, in which its flexible lid-forming loop near the catalytic site was present in open and closed states. We then performed structure-guided mutations of the lid-forming loop, and successfully obtained mutants with higher catalytic activities against a wider range of substrates. Further, we examined the yield of (4*R*,6*R*)-actinol in the one-pot, two-step biocatalytic conversion with the most active CmOYE mutant and LVR, and we observed a significantly higher yield of (4*R*,6*R*)-actinol relative to that obtained with wild-type CmOYE. We also discuss the structural difference of the lid-forming loops in other OYE proteins. The structural and biochemical results in this study provide insights into the molecular basis of the lid-forming loop important for catalytic activity of other OYEs.

## Results and Discussion

### Crystal structures of CmOYE and CmOYE–*p*-HBA

The crystal structures of both CmOYE (403 aa) and a CmOYE–*p*-HBA (*p*-hydroxybenzaldehyde) complex were determined at 1.8 Å resolution (Figure S1 in the Supporting Information; PDB IDs: 4TMB and 4TMC; X-ray diffraction data and structural refinement statistics in Table S1). The crystals of both CmOYE and the CmOYE–*p*-HBA complex contained two CmOYE dimers in an asymmetric unit. Each protomer of CmOYE or CmOYE–*p*-HBA consists of eight  $\alpha$ -helices and eight  $\beta$ -strands, and folds into an  $\alpha_8\beta_8$  barrel (the conserved motif among OYEs) with a bound FMN molecule at the top of the  $\beta$  barrel. The secondary structure elements are shown in Figure S2. The  $\alpha$ -helices

and  $\beta$ -strands forming the  $\alpha_8\beta_8$  barrel are named as shown in Figure S2 (each loop is numbered according to the  $\beta$ -strand it follows). No electron density of NADP<sup>+</sup> in the catalytic site of CmOYE or CmOYE–*p*-HBA was observed, even though a tenfold molar excess of NADP<sup>+</sup> to CmOYE was present in the crystallization drops.

In the absence of *p*-HBA, the electron density of loop 6 was observed only in chain A, possibly because of the formation of intermolecular hydrogen bonds between chains A in adjacent asymmetric units (Table S2). In the presence of bound *p*-HBA, hydrophobic interactions between loop 6 and *p*-HBA contribute to the stable conformation of loop 6, such that electron density for loop 6 was observed for all the chains.

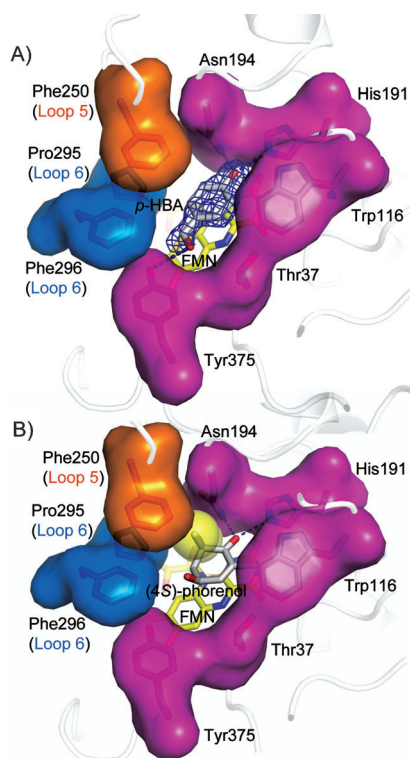
Both CmOYE and the CmOYE–*p*-HBA complex form homodimers through interactions of the  $\alpha_5$  and  $\alpha_6$  helices in the respective crystals; this is consistent with the gel filtration data,<sup>[5]</sup> which showed that CmOYE behaves as a homodimer in solution irrespective of the presence or absence of *p*-HBA. The rmsd between any protomer pair of CmOYE and the CmOYE–*p*-HBA complex range from 0.2 to 1.0 Å (Table S3).

Table S4 lists the hydrogen bonds between CmOYE and FMN. These hydrogen bonds contribute to the orientation of bound FMN, which is oriented in a similar manner to FMNs bound to other OYEs, with its *re* face buried in the protein and its *si* face directed toward the solvent (Figure S1). The amino acid residues involved in the recognition of bound FMN are highly conserved (Figure S3). The bound FMN contains a planar isoalloxazine ring, consistent with the proposal that a methionine residue at the position corresponding to Leu36 in CmOYE would result in a “butterfly” conformation flavin, whereas amino acid residues other than methionine would not.<sup>[14]</sup>

Figure 1A shows the active site of the CmOYE–*p*-HBA complex. The  $F_{\text{obs}} - F_{\text{calcd}}$  electron density map of *p*-HBA is shown in blue mesh contoured at  $2.5\sigma$ . *p*-HBA binds to CmOYE with three hydrogen bonds: O1 in the aldehyde group of *p*-HBA forms a hydrogen bond to the side-chain hydroxyl group of Tyr375, and O4 in the hydroxyl group of *p*-HBA forms hydrogen bonds to NE2 of His191 and ND2 of Asn194. In contrast, no electron density was observed for any substrates used in the co-crystallization. This is probably because these substrates bind less tightly to CmOYE than *p*-HBA, without forming a hydrogen bond with Tyr375.

A comparison of the crystal structures of CmOYEs in the presence and absence of *p*-HBA shows the high flexibility of loop 6. In the presence of bound *p*-HBA, loop 6 adopts a closed conformation in all CmOYE chains, whereas in the absence of bound *p*-HBA, loop 6 is observed only in chain A, where it adopts an unprecedented open conformation (Figure 2). All reported OYE structures show loop 6 adopting the closed conformation. Flexibility of loop 6 was also suggested for *Saccharomyces pastorianus* OYE (SpOYE),<sup>[15]</sup> because NAD(P)H could not access either the catalytic site, or the FMN if the loop adopted only the closed conformation.

To gain insights into the substrate preferences of CmOYE, the binding model of (4*S*)-phorenol to CmOYE was built based on the crystal structures of the CmOYE–*p*-HBA complex (Fig-



**Figure 1.** A) The catalytic site of CmOYE in complex with *p*-HBA. The electron density map OMIT  $|mF_o - DF_c|$  of *p*-HBA (shown both in a stick model and blue mesh contoured to  $2.5\sigma$ ). The amino acid residues shown in orange, blue, and magenta are residues on loop 5, loop 6, and others, respectively. B) Putative binding model of (4*S*)-phorenol to CmOYE. The dimethyl groups at C6 are shown as yellow spheres. The oxygen and carbon atoms in *p*-HBA are red and white, respectively. Dotted lines represent hydrogen bonds.

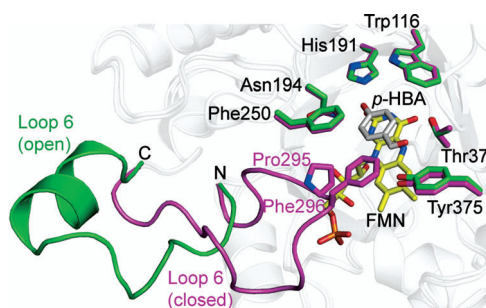


**Figure 2.** Superposition of CmOYE structures in the absence (green) and presence (magenta) of *p*-HBA in the catalytic pockets. The structures shown in green and magenta represent open and closed forms of CmOYE (loop 6), respectively. Amino acid residues in the catalytic sites, FMN (yellow), and *p*-HBA (gray), are shown as stick models.

ures 1 B, S4, and S5). The O, C, C<sup>α</sup>, and C<sup>β</sup> atoms of (4*S*)-phorenol were superimposed onto the position of the O, C, C<sup>α</sup>, and C<sup>β</sup> atoms of *p*-HBA, respectively, as it has been proposed that the position of the carbonyl group of the substrate is trapped by the histidine/asparagine or histidine/histidine pair,<sup>[11]</sup> and that the targeted C=C bond is placed on top of N5 of FMN. The binding model of (4*S*)-phorenol to CmOYE implies that the

bulky dimethyl group at C6 of (4*S*)-phorenol would not be favored by CmOYE, because the dimethyl group at C6 can collide with Pro295 in loop 6 and Phe250 in loop 5 (Figures 1 B and S4).

To examine the effects of Phe250, Pro295, and Phe296 on the substrate preference of CmOYE, mutants F250G, P295G, and F296G were constructed to avoid the possible collision between the dimethyl group in (4*S*)-phorenol and these three residues in CmOYE. The results demonstrated that, compared to wild-type CmOYE, the P295G mutant showed higher catalytic activities toward ketoisophorone and (4*S*)-phorenol. This could be explained by Pro295 colliding with the dimethyl group of ketoisophorone and (4*S*)-phorenol. Thus, Pro295 in loop 6 of CmOYE acts as a substrate filter. Because of the lack of side-chain atoms in Gly and the much greater flexibility of torsion angles ( $\varphi$  and  $\psi$ ) in Gly compared with those in Pro, the P295G mutant has more space in the active site and increased conformational flexibility of loop 6, the lid of the catalytic site. Then we examined the importance of Phe296 in loop 6 by saturation mutations, and demonstrated that this residue has a less significant effect on the catalytic activity than Pro295 (Figure S6).

To investigate further, a series of mutants with polyglycine in loop 6 of CmOYE were constructed, and their catalytic activities were examined. The mutants were named CmOYE-(loop 6→G<sub>*n*</sub>) to indicate a CmOYE mutant in which the loop 6 of CmOYE (<sup>289</sup>EPRVTDPF<sub>L</sub>PEFEKWFKEGT<sup>308</sup>) is replaced with a polyglycine linker G<sub>*n*</sub> (*n* = 2–5). All four mutants exhibited higher catalytic activity toward (4*S*)-phorenol (Figure 3). These results support the hypothesis that the loop 6 plays a significant role in substrate recognition. Although the kinetic parameters of the series of mutants were examined, not all data were obtained because of the low affinity of each mutant toward ketoisophorone and/or (4*S*)-phorenol (Table S5).

The binding model of (4*S*)-phorenol to CmOYE suggests that the bulky dimethyl group at C6 of (4*S*)-phorenol would not be

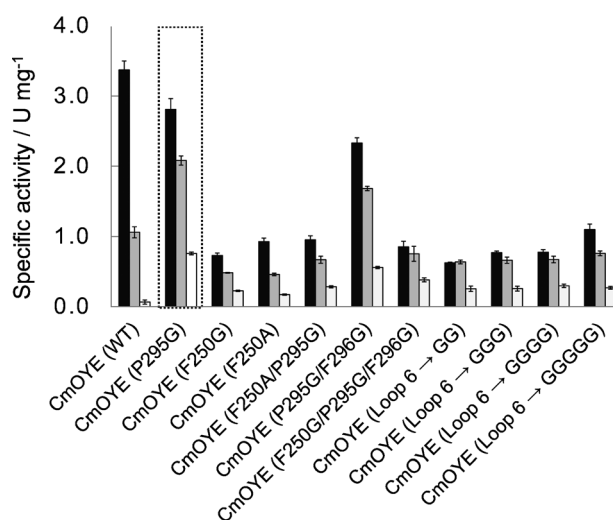


**Figure 3.** Specific activity of CmOYE and its mutants toward cyclohex-2-en-1-one (black), ketoisophorone (gray), and (4*S*)-phorenol (white). It should be noted that specific activity does not reflect binding affinity.

avored by CmOYE, because the dimethyl group in (4S)-phorenol would collide with Phe250 in loop 5 and Pro295 in loop 6 (Figure 1B, Figure S5). This is supported by the fact that CmOYE(F250G) and CmOYE(F250A), both of which should have larger substrate binding pockets than CmOYE(WT), showed increased catalytic activities toward (4S)-phorenol (Figure 3). In contrast, CmOYE(F250A/P295G) and CmOYE(F250G/P295G/F296G), which should have even larger substrate binding pockets than CmOYE(F250G) and CmOYE(F250A), showed less catalytic activities towards cyclohex-2-en-1-one, ketoisophorone, and (4S)-phorenol (Figure 3), thus suggesting that these substrate-binding pockets are too big. We chose CmOYE(P295G), which showed two- and 12-fold higher catalytic activities toward ketoisophorone and (4S)-phorenol, respectively, than the wild-type enzyme, as the most suitable enzyme for the efficient biocatalytic conversions of ketoisophorone to (6R)-levodione and (4S)-phorenol to (4R,6R)-actinol.

The time-courses of the production of (6R)-levodione, (4S)-phorenol, and (4R,6R)-actinol from ketoisophorone in the one-pot two-step biocatalytic conversion by CmOYE(WT) or CmOYE(P295G) with LVR are shown in Figure 4. The conversion

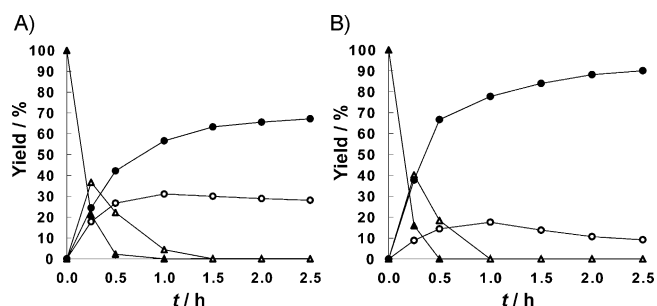


**Figure 4.** Time-course of the production for (6R)-levodione ( $\Delta$ ), (4S)-phorenol ( $\circ$ ), and (4R,6R)-actinol ( $\bullet$ ) from ketoisophorone ( $\blacktriangle$ ) in a simultaneous two-step biocatalytic conversion by A) CmOYE(WT) and B) CmOYE(P295G). The reactions were stopped when the yields of (4R,6R)-actinol approached the plateau phase (2.5 h).

by CmOYE(P295G) and LVR showed a higher yield of (4R,6R)-actinol than by CmOYE(WT) and LVR. After 2.5 h, CmOYE(WT) and LVR produced (4R,6R)-actinol in 67.2% yield with 28.1% accumulation of the (4S)-phorenol intermediate, whereas CmOYE(P295G) and LVR produced (4R,6R)-actinol in 90.1% yield with only 9.1% accumulation of (4S)-phorenol. These results demonstrate that introducing mutations into loop 6 (the lid of the catalytic site) enhances the catalytic activities of CmOYE with (4S)-phorenol, and contributes to the significant improvement in the yield of (4R,6R)-actinol in the one-pot, two-step biocatalytic conversion.

Ketoisophorone (compound D in Figure S7) is a good substrate for CmOYE(WT); it has two carbonyl groups that would be recognized by the His191/Asn194 pair of CmOYE. To examine the modes of recognition of ketoisophorone by CmOYE, the catalytic activities toward cyclohex-2-en-1-one, 3-methylcyclohex-2-en-1-one, isophorone, and ketoisophorone were examined (Figure S7). No catalytic activity of CmOYE was detected toward 3-methylcyclohex-2-en-1-one or isophorone (com-

pounds B and C in Figure S7), both of which have a 3-methyl group, whereas some catalytic activity was detected toward ketoisophorone and cyclohex-2-en-1-one (compounds D and A in Figure S7), both of which lack a 3-methyl group, thus suggesting that ketoisophorone and cyclohex-2-en-1-one enter the catalytic pocket of CmOYE in a similar orientation. In other words, the carbonyl group at position 1 of ketoisophorone is equivalent to the carbonyl group of cyclohex-2-en-1-one when recognized by CmOYE. The molecular model constructed based on the crystal structure of CmOYE indicates that the 3-methyl group of 3-methylcyclohex-2-en-1-one and isophorone would collide with Thr37 and Trp116 in CmOYE (Figure S8), thus clearly explaining why these compounds are not suitable substrates for CmOYE.

### Mutation in loop 6 can alter the substrate specificity of OYEs

Based on crystallographic data, the structures of the catalytic sites of OYEs can be divided into two groups: the CmOYE family and BsOYE family. In the case of the CmOYE family, loop 6 acts as a mobile lid of the catalytic site, whereas in the BsOYE family, loop 6 is a relatively rigid loop (Figure 5). Based on this structural classification, *C. macedoniensis* OYE (CmOYE; PDB ID: 4TMB; this study), *S. pastorianus* OYE (SpOYE; PDB ID: 1OYB),<sup>[15]</sup> and *Shewanella oneidensis* OYE (SoOYE; PDB ID: 2GQ9)<sup>[14]</sup> belong to the CmOYE family; *Bacillus subtilis* OYE (BsOYE, also known as YqjM; PDB ID: 1Z42),<sup>[16]</sup> *Thermus scotoductus* SA-01 OYE (TsOYE, also known as CrS; PDB ID: 3HGJ)<sup>[17]</sup> and *Pseudomonas putida* xenobiotic reductase A (XenA; PDB ID: 3L66)<sup>[18]</sup> belong to the BsOYE family. OYE can be used for highly stereo-selective reduction, but an (R)-enantiomer of 6-membered cyclic enone has not been yet obtained with OYE.

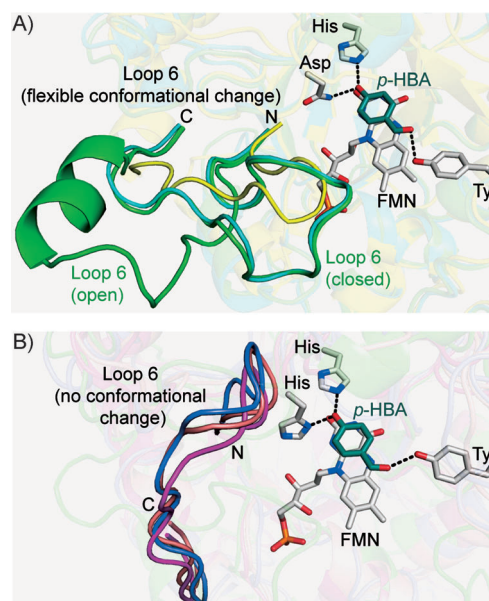


**Figure 5.** Catalytic site and loop 6 of A) the CmOYE family and B) the BsOYE family. CmOYE, SpOYE, SoOYE, BsOYE, TsOYE, and XenA are shown in green, cyan, yellow, magenta, brown and blue, respectively.

In a previous study, an iterative saturation mutagenesis (ISM) method<sup>[1]</sup> was applied to expand the substrate range of BsOYE by using 3-methylcyclohex-2-en-1-one as a model substrate.<sup>[19]</sup> However, the results in our study indicated that not only BsOYE-family but also CmOYE-family proteins would be candidates for ISM to increase the catalytic activities toward 3-methylcyclohex-2-en-1-one and to control the *R* and *S* selectivities.

## Conclusion

We first aimed to establish a biocatalytic method for the synthesis of (4*R*,6*R*)-actinol (an important carotenoid precursor) from a commercially available compound, and found that a two-step conversion from ketoisophorone to (4*R*,6*R*)-actinol is possible by using the two enzymes CmOYE and LVR, both of which showed high enantioselectivity. However, the one-pot two-step conversion with a mixture of these enzymes gave only 67.2% yield of (4*R*,6*R*)-actinol. As this low yield was a result of the narrow substrate preference of CmOYE, we then aimed to create an artificial CmOYE with higher activity toward a broader range of substrates, by characterizing a flexible region of CmOYE near the catalytic site. We first solved the crystal structures of CmOYE in the absence and presence of *p*-HBA (a substrate analogue) to visualize the substrate recognition mechanism of CmOYE. We observed two different states of loop 6 (open and closed states, in the absence and presence of *p*-HBA, respectively) and found that this loop acts as a lid at the catalytic site. Based on the ligand-free and ligand-bound structures, we propose that Pro295 and Phe296 in loop 6 as well as Phe250 in loop 5 are key residues in substrate recognition, and are amenable to mutational analysis. We found that CmOYE(P295G) shows 2- and 12-fold higher catalytic activity toward ketoisophorone and (4*S*)-phorenol, respectively, than the wild-type enzyme, and significantly improved the yield of (4*R*,6*R*)-actinol (from 67.2 to 90.1%) in a one-pot two-step transformation.

Notably, the CmOYE variants lacking the lid-forming loop showed higher and lower catalytic activity toward (4*S*)-phorenol and 3-methylcyclohex-2-en-1-one, respectively, thus suggesting that the lid-forming loop of CmOYE acts as a substrate filter. Comparisons of catalytic sites of CmOYE-family and BsOYE-family proteins revealed notable structural differences: CmOYE-family proteins have flexible lid-forming loops, whereas BsOYE-family proteins have no lid-forming loops (Figure 5). This observation agrees with the hypothesis that *in vivo* substrates of CmOYE-family proteins and BsOYE-family proteins are different, although it needs to be considered whether the lids of CmOYE-family proteins evolved primarily for optimizing turnover rates of NAD(P)H and substrates. From an industrial point of view, the observation that loop 6 in OYEs acts as a substrate filter is of great interest for the development of novel OYE biocatalysts.

## Experimental Section

**Protein expression and purification:** The gene encoding CmOYE was amplified by PCR using the cloned CmOYE gene as the tem-

plate.<sup>[7]</sup> The PCR primers used were 5'-CGCGC GCGCA TATGA AAAAC AATAA AGAAC GACAA GGAAA-3' (including an NdeI site, underlined) and 5'-GGGGC CCCGG ATCCT TATTA AGAGA GGGGA AGGTG CACTT CA-3' (including a BamHI site, underlined). The PCR product was digested with NdeI and BamHI, and ligated into the expression vector pET-28a(+) (Novagen). The point and deletion mutants were introduced by site-directed mutagenesis using the pET-28a plasmid. To obtain CmOYE with a thrombin-cleavable N-terminal His<sub>6</sub>-tag, *Escherichia coli* BL21(DE3) harboring the expression plasmid was grown at 37 °C in LB medium, and protein expression was induced by adding IPTG (1 mM) and further incubating at 37 °C for 3 h. Cells were harvested by centrifugation, resuspended in lysis buffer (Tris-HCl (50 mM, pH 8.0), NaCl (300 mM), imidazole (10 mM)), and disrupted by sonication on ice. After centrifugation, CmOYE with an N-terminal His<sub>6</sub>-tag was purified with Ni Sepharose 6 Fast Flow (GE Healthcare). The His<sub>6</sub> tag was removed by thrombin protease (Novagen) digestion. CmOYE was further purified by anion exchange chromatography with a Resource Q 6 mL column, followed by size exclusion chromatography with a Superdex 200 HR 10/30 column (GE Healthcare). The purified sample was then concentrated (~10 mg mL<sup>-1</sup>) in a 20 mL Vivaspin concentrator (10 kDa cutoff; Sartorius, Göttingen, Germany). The protein concentration was determined based on absorbance ( $\epsilon_{280} = 8940 \text{ M}^{-1} \text{ cm}^{-1}$ ) obtained with a NanoDrop ND-1000 spectrophotometer (Thermo Scientific).

**Crystallization and data collection:** Crystallization experiments were performed with the sitting drop vapor diffusion method at 293 K. Crystals of CmOYE and CmOYE-*p*-HBA were obtained by mixing protein (1.0  $\mu\text{L}$ , 10 mg mL<sup>-1</sup>) with NADP<sup>+</sup> (5 mM) with/without *p*-HBA (5 mM; Sigma-Aldrich) in a reservoir solution (1.0  $\mu\text{L}$ ) containing PEG 3350 (25%, v/v), Tris-HCl (100 mM, pH 8.0), and ammonium sulfate (200 mM). Diffraction data were collected at NW-12 A at PF-AR (Ibaraki, Japan). Data processing was carried out with the programs HKL2000<sup>[20]</sup> and XDS.<sup>[21]</sup> Crystals of CmOYE belong to space group C2 with unit cell dimensions  $a = 287.5 \text{ \AA}$ ,  $b = 59.6 \text{ \AA}$ ,  $c = 100.3 \text{ \AA}$ , and  $\beta = 109.9^\circ$ ; crystals of CmOYE-*p*-HBA belong to space group P2<sub>1</sub>2<sub>1</sub>2<sub>1</sub> with unit cell dimensions  $a = 52.3 \text{ \AA}$ ,  $b = 150.9 \text{ \AA}$ , and  $c = 199.7 \text{ \AA}$ . The asymmetric units for both CmOYE and CmOYE-*p*-HBA contained four molecules.

**Structure determination of CYE and the CYE-*p*-HBA complex:** The structures of CmOYE and CmOYE-*p*-HBA were determined by molecular replacement with the program MolRep<sup>[22]</sup> with the atomic coordinates of *S. pastorianus* OYE (SpOYE; PDB ID: 1OYA; 69% sequence identity to CmOYE) as the initial model. Further model building and refinements were performed with the programs ARP/wARP,<sup>[23]</sup> Coot,<sup>[24]</sup> and Refmac.<sup>[25]</sup> FMN, *p*-HBA, and water molecules were modeled in the final stages of refinement based on the  $F_{\text{obs}} - F_{\text{calc}}$  electron density map. The refined structure of CmOYE was used as the template for the molecular replacements of the CmOYE-*p*-HBA. The refined structures were visualized with PyMol (<http://pymol.sourceforge.net/>). To evaluate the structural similarity, the Dalilite server<sup>[26]</sup> was used to calculate the rms deviations of protomers among OYEs. The STRAP program was used for structure-based sequence alignment (<http://www.bioinformatics.org/strap/>).

**Catalytic activities:** Cyclohex-2-en-1-one and 3-methylcyclohex-2-en-1-one were purchased from Wako Pure Chemical Industries (Osaka, Japan); ketoisophorone and (4*S*)-phorenol were from Nippon-Roche Co. (Tokyo, Japan); and menadiolone was from Nacalai Tesque Inc. (Kyoto, Japan). Catalytic activity was examined in Tris-HCl (200 mM, pH 7.5, 0.5 mL) containing NADPH (0.32 mM, cofactor) and an appropriate amount of the wild-type or mutant

CmOYE (enzyme). After 2 min of incubation at 303 K without substrate, the reaction was started by addition of substrate (cyclohex-2-en-1-one (4 mM), ketoisophorone (4 mM), (4S)-phorenol (4 mM), 3-methylcyclohex-2-en-1-one (4 mM), or menadione (0.2 mM)), and then the decrease in absorbance at 340 nm was monitored at 303 K. One unit (1 U) of enzyme activity was defined as the amount catalyzing the oxidation of 1  $\mu\text{mol}$  of NADPH per minute. The enzyme activity of the wild-type CmOYE was used as the reference. The kinetics parameters were calculated by using the same method described above with a variety of substrate concentrations.

**Enzymatic production:** Recombinant cells that overproduce LVR,<sup>[27]</sup> CmOYE(WT), or CmOYE(P295G) were suspended in Tris-HCl buffer (20 mM, pH 7.4), and then disrupted by sonication on ice. The supernatant after centrifugation was used as a cell-free extract. The amount of wild-type or mutant CmOYE in cell-free extract was determined by using cyclohex-2-en-1-one as the substrate. Enzymatic production was examined in a 2.5 mL reaction mixture containing ketoisophorone (6.6 mM 1 mg mL<sup>-1</sup>; substrate), NADH (20 mM; cofactor), NADPH (10 mM; cofactor), cell-free extract (containing 0.8 mg of CmOYE(WT) or CmOYE(P295G), enzyme amount calculated based on the specific activity with cyclohex-2-en-1-one), cell-free extract containing LVR (0.2 U; enzyme amount calculated based on the specific activity for (6R)-levodione), of glucose dehydrogenase (40 U), and glucose (278 mM) in potassium phosphate buffer (200 mM, pH 7.0). The mixture was incubated at 30 °C for 2.5 h. The concentrations of the substrate and products were measured by gas chromatography as described previously.<sup>[7]</sup>

## Acknowledgements

We thank the beamline staff at Photon Factory for their kind help with the data collection, Dr. Yusuke Ogura and Dr. Keisuke Yamamoto for sincere discussion, Dr. John Salvatore Scotti for help revising the manuscript. The synchrotron-radiation experiments were done with the approval of Photon Factory, KEK (2009G199). This work was supported in part by the National Project on Protein Structural and Functional Analyses, the Targeted Proteins Research Program, the Platform for Drug Discovery, Informatics, and Structural Life Sciences, and Grants-in-Aid for Scientific Research from the Ministry of Education, Culture, Sports, Science, and Technology of Japan.

**Keywords:** biocatalysis · enzyme catalysis · enzymes · old yellow enzyme · X-ray crystallography

- [1] M. T. Reetz, J. D. Carballeira, *Nat. Protoc.* **2007**, *2*, 891–903.
- [2] M. Hall, C. Stueckler, H. Ehammer, E. Pointner, G. Oberdorfer, K. Gruber, B. Hauer, R. Stuermer, W. Kroutil, P. Macheroux, K. Faber, *Adv. Synth. Catal.* **2008**, *350*, 411–418.
- [3] S. K. Padhi, D. J. Bougioukou, J. D. Stewart, *J. Am. Chem. Soc.* **2009**, *131*, 3271–3280.
- [4] M. Wada, A. Yoshizumi, Y. Noda, M. Kataoka, S. Shimizu, H. Takagi, S. Nakamori, *Appl. Environ. Microbiol.* **2003**, *69*, 933–937.
- [5] M. Kataoka, A. Kotaka, A. Hasegawa, M. Wada, A. Yoshizumi, S. Nakamori, S. Shimizu, *Biosci. Biotechnol. Biochem.* **2002**, *66*, 2651–2657.
- [6] K. Stott, K. Saito, D. J. Thiele, V. Massey, *J. Biol. Chem.* **1993**, *268*, 6097–6106.
- [7] M. Kataoka, A. Kotaka, R. Thiwthong, M. Wada, S. Nakamori, S. Shimizu, *J. Biotechnol.* **2004**, *114*, 1–9.
- [8] M. Wada, A. Yoshizumi, S. Nakamori, S. Shimizu, *Appl. Environ. Microbiol.* **1999**, *65*, 4399–4403.
- [9] S. Sogabe, A. Yoshizumi, T. A. Fukami, Y. Shiratori, S. Shimizu, H. Takagi, S. Nakamori, M. Wada, *J. Biol. Chem.* **2003**, *278*, 19387–19395.
- [10] R. E. Williams, N. C. Bruce, *Microbiology* **2002**, *148*, 1607–1614.
- [11] B. J. Brown, Z. Deng, P. A. Karplus, V. Massey, *J. Biol. Chem.* **1998**, *273*, 32753–32762.
- [12] R. M. Kohli, V. Massey, *J. Biol. Chem.* **1998**, *273*, 32763–32770.
- [13] B. J. Brown, J.-W. Hyun, S. Duvvuri, P. A. Karplus, V. Massey, *J. Biol. Chem.* **2002**, *277*, 2138–2145.
- [14] D. van den Hemel, A. Brigé, S. N. Savvides, J. Van Beeumen, *J. Biol. Chem.* **2006**, *281*, 28152–28161.
- [15] K. M. Fox, P. A. Karplus, *Structure* **1994**, *2*, 1089–1105.
- [16] K. Kitzing, T. B. Fitzpatrick, C. Wilken, J. Sawa, G. P. Bourenkov, P. Macheroux, T. Clausen, *J. Biol. Chem.* **2005**, *280*, 27904–27913.
- [17] D. J. Opperman, B. T. Sewell, D. Litthauer, M. N. Isupov, J. A. Littlechild, E. van Heerden, *Biochem. Biophys. Res. Commun.* **2010**, *393*, 426–431.
- [18] O. Spiegelhauer, S. Mende, F. Dickert, S. H. Knauer, G. M. Ullmann, H. Dobbek, *J. Mol. Biol.* **2010**, *398*, 66–82.
- [19] D. J. Bougioukou, S. Kille, A. Taglieber, M. T. Reetz, *Adv. Synth. Catal.* **2009**, *351*, 3287–3305.
- [20] Z. Otwinowski, W. Minor, *Methods Enzymol.* **1997**, *276*, 307–326.
- [21] W. Kabsch, *J. Appl. Crystallogr.* **1993**, *26*, 795–800.
- [22] A. Vagin, A. Teplyakov, *Acta Crystallogr. Sect. D Biol. Crystallogr.* **2000**, *56*, 1622–1624.
- [23] A. Perrakis, M. Harkiolaki, K. S. Wilson, V. S. Lamzin, *Acta Crystallogr. Sect. D Biol. Crystallogr.* **2001**, *57*, 1445–1450.
- [24] P. Emsley, K. Cowtan, *Acta Crystallogr. Sect. D Biol. Crystallogr.* **2004**, *60*, 2126–2132.
- [25] A. A. Vagin, R. A. Steiner, A. A. Lebedev, L. Potterton, S. McNicholas, F. Long, G. N. Murshudov, *Acta Crystallogr. Sect. D Biol. Crystallogr.* **2004**, *60*, 2184–2195.
- [26] L. Holm, J. Park, *Bioinformatics* **2000**, *16*, 566–567.
- [27] A. Yoshizumi, M. Wada, H. Takagi, S. Shimizu, S. Nakamori, *Biosci. Biotechnol. Biochem.* **2001**, *65*, 830–836.

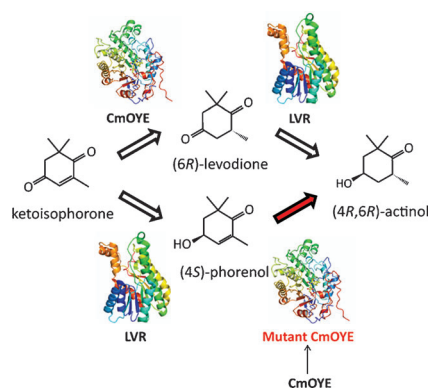
Received: September 23, 2014

Published online on ■ ■ ■ ■, 0000

## FULL PAPERS

### Crystal structures of old yellow enzyme from *C. macedoniensis* (CmOYE)

identify a flexible lid-forming loop, which is revealed to be important for substrate recognition. The yield of (4*R*,6*R*)-actinol was improved from 67.2 to 90.1 % in a one-pot, two-step biocatalytic reduction system, by introducing mutations into this loop. Our results will be of use in developing new OYE biocatalysts.



S. Horita, M. Kataoka, N. Kitamura, T. Nakagawa, T. Miyakawa, J. Ohtsuka, K. Nagata, S. Shimizu, M. Tanokura\*

■■■ - ■■■

**An Engineered Old Yellow Enzyme that Enables Efficient Synthesis of (4*R*,6*R*)-Actinol in a One-Pot Reduction System**

